2017 7th International Conference on Power Systems (ICPS)
College of Engineering Pune, India. Dec 21-23, 2017

Assessment of Harmonic Distortion on Distribution Feeders with Electric Vehicles and Residential PVs

Oğuzhan Ceylan
Assistant Professor
Kadir Has University
Istanbul, Turkey
Email: oguzhan.ceylan@khas.edu.tr

Sumit Paudyal
Assistant Professor
Michigan Tech. University
Houghton, MI, USA
Email: sumitp@mtu.edu

Sudarshan Dahal
Development Engineer
Powerlink Queensland
Virginia, QLD, Australia
Email: sdahal@powerlink.com.au

Nava R. Karki
Professor
Tribhuvan University
Kathmandu, Nepal
Email:nkarki@ioe.edu.np

***Abstract*—Power-electronic interfacing based devices such as photovoltaic (PV) panels and electric vehicles (EVs) cause voltage/current harmonic distortions on the power grid. The harmonic current profiles from EVs and PVs depend on the design of the controllers integrated to the PV inverters and EV chargers. Similarly, the voltage and current harmonic distortions on a grid change throughout the day as the PV output power, number of grid connected EVs, and the other load pattern change. In this context, we present harmonic assessment to demonstrate cumulative effect of large number of EVs and PVs on a medium voltage distribution grid. We will demonstrate the case studies on the IEEE 123-node distribution feeder with 20%, 50%, and 100% PV and EV penetrations, based on time series simulations carried out for an entire day.**

***Index Terms*—Electric Vehicles, Photovoltaics, Distribution Grid, Total Harmonic Distortion, Power Quality**

I. Introduction

Electric vehicles (EVs) and photovoltaic (PV) systems provide economic and environmental benefits, which motivate large scale adoption of the technologies in residential energy distribution systems. EVs and solar power have capability to help reduce the emissions and depletion of fossil fuels. However, the EV and PV technologies have some downsides as well. Integration of EVs and PVs in the power network causes adverse impacts due to the increased load from EV charging, and reverse power flow and intermittency of solar power [1], [2]. The placement and number of EV loads and PVs impact the voltage profile in the power distribution network. Similarly, studies have shown that uncoordinated charging of EVs leads to increased peak demand, which impacts the overall reliability of the grid [3]. Also, the presence of PVs and EVs cause power quality issues including harmonic distortions in power grids.

The EVs and PVs connect to the grid through power-electronic interfacing devices (i.e., PV inverters and EV chargers), which make the EVs/PVs function as nonlinear devices. Therefore, integration of EVs/PVs on the grid causes current and voltage harmonic distortions. The harmonic profile of the devices depends on several factors including the design of the controllers in the inverters and chargers, and hence it widely varies across the manufacturers. With the advancements on technology, the current total harmonic distortion (THD_i) from individual EV chargers is rapidly going down. For example, the chargers from 1993 show an average THD_i value of 50%, while the average THD_i level on EV chargers from 1995 is 6.12% [4]. Based on the current limits for individual harmonic in IEC standard [5], the maximum THD_i allowed for an individual EV charger would be 17.3% [6]. IEEE Standard [7] defines – THD_i limit caused by an individual load should be less than 15% for upto 11^{th} harmonics [8]. On the voltages, IEEE Standard [7] defines limit of 3% for individual voltage distortion and 5% for total harmonic distortion (THD_v) for voltage level less than 69 kV [9].

Harmonic currents cause abnormal operation including increased power losses, temperature rise, premature insulation failure, and winding failure of transformers [10]– this can cause adverse impacts on reliability, security, and efficiency of the power grid. Previous studies carried out in [8], [10]–[13] find the impact of harmonics due to the integration of EVs. For example, based on [8], lost in transformer life depends on THD_i and the relation is quadratic. Reference [8] also suggests that THD_i should be limited to 25–30% for better transformer life.

Two charging schemes are considered in [11] to analyze the adverse impacts of EVs. In the uncoordinated random charging scenario, maximum node voltage deviation and poor power quality are observed. However, power losses and THD_v are found much less in the case of coordinated charging of EVs. In [11], it is also demonstrated that when the EV penetration is low, THDs are not significant and the scenario is not concerning to the utilities. Similar conclusion is made in [14] that low EV penetration may not cause significant impact on THDs. Reference [15] evaluates harmonic distortion and voltage drop considering different EV penetration levels and with various charging strategies. It is observed that power quality issue becomes concerning when the EV penetration level exceeds 45%. Reference [15] also evaluates THD_v with THD_i of 17.4% for individual EVs, and it is found that voltage THD_v can go as high as 14.2% on low voltage (LV) network with mutiple EVs. Based on [16], THD_v on the secondary of service transformer should not be an issue if EVs operate at power factor of 95% and THD_i less than 20%.

Harmonic profiles of EVs and PVs are also time varying quantities. Reference [17] shows EV charging process where

978-1-5386-1789-2/17/$31.00 ©2017 IEEE

the THD_i at the beginning of charging is below 5.26%, while the THD_i reaches to 28% at the end of the charging. Another study in [9] shows quite different observation that the THD_i increases up to 45% in the beginning of the charging process, then it achieves fairly constant values between 11.5-12.5%, and increases again towards the end of the charging process.

Similarly, harmonic profile of PVs depend on the design of inverters and several other factors including the solar insolation. Reference [18] shows that the current regulated current source inverter (CRCSI) and current controlled voltage source inverter (CCVSI) exhibit different harmonic patterns. Reference [19] studies the variation of harmonic distortions due to PV plant when the solar insolation changes. The THD_i during sunrise and sunset can be as high as 50% when the third harmonic current shows peak values. In overcast days, THD_i can vary between 17.65 to 50%. However, it is observed in [19] that THD_v is not affected by the solar insolation and is observed below 2%.

At the aggregation level, the impact of EVs and PVs on THDs would not be simply additive. Due to the diversity of chargers and inverters available in the market, harmonic cancellation can take place to certain extent [9]. Reference [20] presents harmonic cancellation effect using Monte Carlo Simulation for the aggregation of EV chargers. Some of the past studies focus on optimal planning and dispatch of distributed generators (DGs) and EVs considering the harmonic distortion. In [21], a multi-objective programming and decision theory based approach is used to solve voltage quality and THD issues with the help of DGs. Similar studies are carried out in [22]–[24], where Particle Swarm Optimization (PSO) is used for optimal siting and sizing of DGs with objectives to reduce THDs and to improve voltage profiles in the grid.

In the context that THDs change throughout a day and depend on the penetration of EVs/PVs, this paper provides an assessment of daily THD profiles on a medium voltage distribution grid considering three different penetration levels of EVs and PVs. The rest of the paper is organized as following. Section II develops the harmonic power flow model necessary to evaluate the THDs, Section III presents the case studies and discussion, and Section IV draws the main conclusions observed from the simulation case studies.

II. Modeling

A. Harmonic Power Flow (HPF) Model

For the harmonic power flow calculation, harmonic decoupled approach is considered as in [25]–[27]. Figure 1 shows the connection of series and shunt elements, which is the basis of building the harmonic power flow (HPF) model.

At harmonic frequencies, the system is modeled using passive elements and harmonic current sources. The impedance of the conductors, cables, and transformers are modified based on the frequencies of interest following the models explained in [28]. The following frequency dependent A, B, C, D parameter matrices derived from the

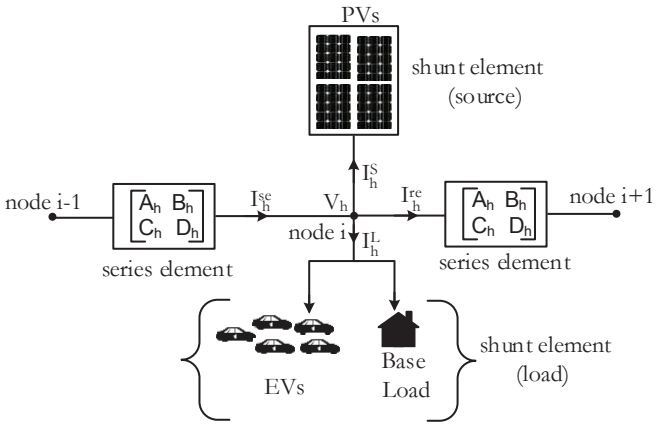

Fig. 1. Circuit connection showing the branch currents and nodal voltages used for modeling the harmonic power flow.

line parameters are used to relate sending and receiving end voltages and currents similar to [29],

$$\begin{bmatrix} V_{i,p,h} \\ I_{se,j,p,h} \end{bmatrix} = \begin{bmatrix} A_{j,p,h} & B_{j,p,h} \\ C_{j,p,h} & D_{j,p,h} \end{bmatrix} \begin{bmatrix} V_{i+1,p,h} \\ I_{re,j,p,h} \end{bmatrix} \tag{1}$$

where subscripts i, j, p, se, re, h represent node, branch connecting node i and $i+1$, phase, sending end, receiving end, and harmonic frequency, respectively. V and I represent three-phase complex voltages and currents, respectively.

The A, B, C, D parameter matrices of conductors, cables, transformers are not time varying except for the transformer load tap changers (LTCs). A, B, C, D matrices for the LTCs depend on the tap position, which can be written as,

$$\left[A_{jl,p,h}\right] = \begin{bmatrix} 1+\Delta Stap_{jl} & 0 & 0 \\ 0 & 1+\Delta Stap_{jl} & 0 \\ 0 & 0 & 1+\Delta Stap_{jl} \end{bmatrix} \tag{2}$$

$$\left[B_{jl,p,h}\right] = \left[C_{jl,p,h}\right] = 0 \tag{3}$$

$$\left[D_{jl,p,h}\right] = \left[A_{jl,p,h}\right]^{-1} \tag{4}$$

where $jl \in j$ represents the LTC branches and $tap \in [-16, 16]$ represents tap position. ΔS represents per unit voltage change due to one tap position. In equation (2), the tap is assumed the same for all phases and is also independent of the frequency of interest.

In this study, only the constant current model is considered, i.e., harmonic loads are modeled as constant current withdrawals and harmonic sources are modeled as constant current sources. This can be represented by the following equations,

$$\left|I^L_{il,p,h}\right| \left(\angle V_{il,p,h} - \angle I^L_{il,p,h}\right) = \left|Io^L_{il,p,h}\right| \angle \theta^L_{il,p,h} \tag{5}$$

$$\left|I^S_{is,p,h}\right| \left(\angle V_{is,p,h} - \angle I^S_{is,p,h}\right) = -\left|Io^S_{is,p,h}\right| \angle \theta^S_{is,p,h} \tag{6}$$

where $il \in i$ represents node in distribution feeder where loads are connected. Similarly, $is \in i$ represents node where sources are connected. I^L and I^S represent harmonic load and source current, respectively. Io^L represents magnitude of harmonic

load current at nominal voltage and θ^L represents power factor angle of harmonic load. Similarly, Io^S represents magnitude of harmonic source current at nominal voltage and θ^S represents power factor angle of harmonic source.

At each node, phase, and for each harmonic frequency a current balance equation is used as following,

$$I_{se,j,p,h} = I_{re,j,p,h} + I^L_{i,p,h} + I^S_{i,p,h} \qquad \forall\ i,p,h \qquad (7)$$

where $il \in i$ represents node in distribution feeder where loads are connected. Equations (1)-(7) represent HPF model.

After HPF model is solved, voltage and current THDs can be computed from the nodal current and voltage information as [30],

$$THD^V_{i,p} = \frac{\left[\sum_{h=2}^{\infty} |V_{i,p,h}|^2\right]^{\frac{1}{2}}}{|V_{i,p,h=1}|} \qquad (8)$$

$$THD^I_{i,p} = \frac{\left[\sum_{h=2}^{\infty} |I_{i,p,h}|^2\right]^{\frac{1}{2}}}{|I_{i,p,h=1}|} \qquad (9)$$

B. Modeling of Base Load, EVs, and PVs

Base loads, EVs, and PVs are modelled as constant current source/loads in the HPF model. Fig. 2 shows the variation of base load profile (normalized), power consumption of one EV, and output profile of one PV used in the simulation. EV consumption profile is obtained using method similar to [31], where an optimization is run to schedule customer's EV based on dynamic energy price and customer's and battery's constraints. EVs are assumed connected to the grid in the morning and after evening, and most of the charging of EVs takes place at night when the energy prices are less expensive. The flat power profile of EV during night is due to the socket rating. PV capacity of 4 $\mathrm{kW_p}$ is assumed, and the output profile in Fig. 2 corresponds to a slight cloudy day.

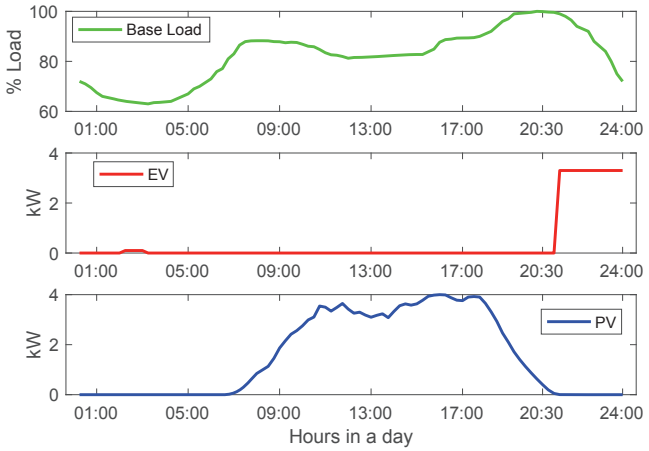

Fig. 2. Normalized base load profile, power consumption profile of one EV, and generation profile of one residential PV.

Fig. 3 shows harmonic profiles used for the simulation case studies. Harmonic currents up to the 40^{th} harmonic are considered. Base load is assumed to have $\mathrm{THD_i}$ of 8.24% [32] at peak load. EV charger's harmonic profile is obtained from [20], [30], which results in $\mathrm{THD_i}$ of 31.94% at peak EV charging load. For the PVs, harmonic profile from [33] is used, which results in $\mathrm{THD_i}$ of 4.99 at peak generation %.

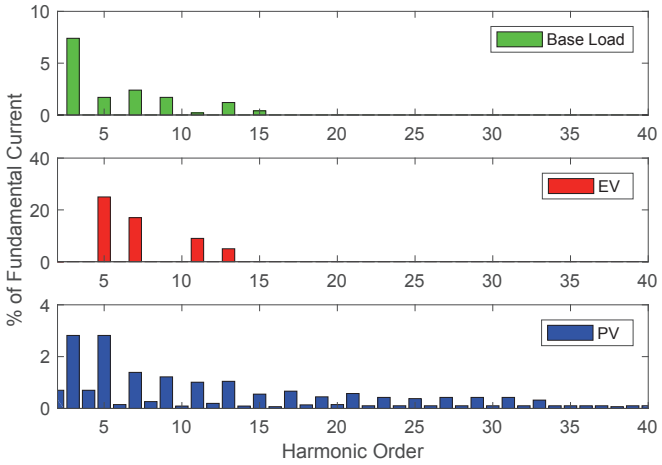

Fig. 3. Harmonic profile ($h = 2^{\mathrm{nd}}$ to 40^{th} order) of currents for base loads, EVs, and PVs.

III. Case Studies

HPF model is implemented in OpenDSS [34] and solved for 4.16 kV IEEE 123-node test feeder [35], [36]. The model in OpenDSS is interfaced with MATLAB for easy data exchange. Topology of the test feeder is shown in Fig. 4 where red colored nodes represent nodes with loads, EVs, and PVs.

Simulations were carried out considering three different penetration levels for EVs and PVs, i.e. high, medium, and low penetration levels. High penetration represents 100% penetration of EVs and PVs. In this case, total number of EVs is 517, and total number of PVs is 411. Similarly, medium and low penetration levels represent 20% and 50% penetration levels, respectively. Simulation results for all these three cases are discussed next.

A. Low Penetration

This case uses only 20% of the PVs and 20% EVs in the simulations. Due to space constraints, simulation results for only two nodes are presented. The first one is a single phase node (phase-a) far from the substation, i.e., node 46, second one is a three phase node closer to substation, i.e., node 7. Fig. 5 shows the daily change of the voltage total harmonic distortion ($\mathrm{THD_v}$) at node 46. The solid line represents the $\mathrm{THD_v}$ for a base case, and dotted line represents the case with penetration levels of EVs and PVs. It can be observed that the changes in the harmonics are in concordant to the daily EV charging and PV output profiles given in Fig. 2.

The daily change of the current total harmonic distortion $\mathrm{THD_i}$ on line 45-46 for base case load and 20% penetration levels of EVs and PVs are given in Fig. 6. The solid and dotted lines represent daily changes of $\mathrm{THD_i}$ for base case load, and low penetration level, respectively. It can be observed that the change in harmonics due to PVs and EVs do not change the

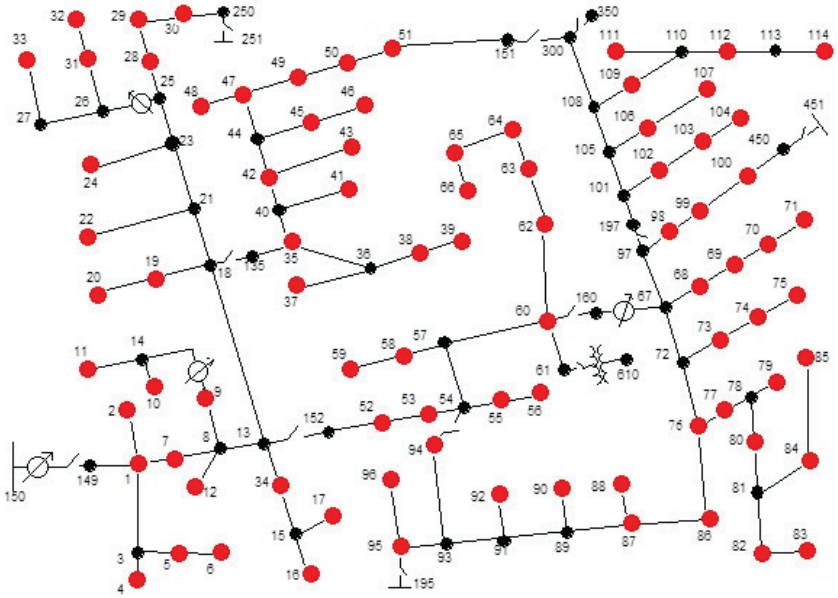

Fig. 4. IEEE 123-node distribution feeder for harmonic analyses [35], [36].

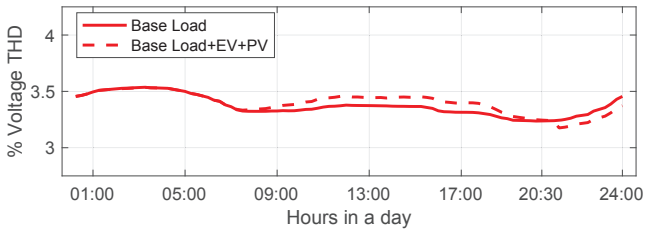

Fig. 5. Node 46 daily change of THD_v low penetration level.

order of the maximum and minimum values of the harmonic profiles. Profile values are slightly changing around 3.5% and 10% for THD_v and THD_i throughout the day.

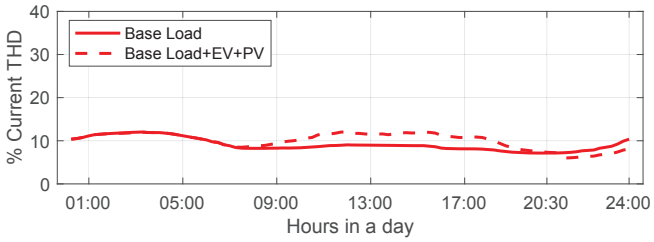

Fig. 6. Line 45-46 daily change of THD_i for low penetration level.

Fig. 7 shows the daily change of 3 phase THD_v on node 7 for base case and 20% penetration levels. Since node 7 is closer to substation compared to node 46, THD_v of node 7 is less than node 46 throughout the day. It can be observed that voltage and current harmonics are increased when PVs are injecting power. However, they are decreased when EVs are charging at both nodes. This is particularly due to the definition of THD, in which fundamental qualities are used in denominator and the fundamental current due EVs is increased relatively more compared to other harmonics. It is obvious from the figure that the level of THD_v of node 7 is approximately 4 times less compared to that of node 46 due to the proximity to the substation.

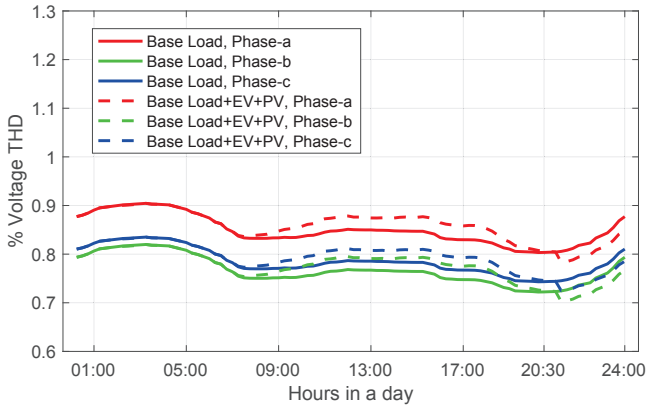

Fig. 7. Node 7 daily change of THD_v for 3 phases, low penetration level.

B. Medium Penetration

This case uses 50% of the PVs and 50% EVs in the simulations. The simulation results are provided for node 46 and node 7. Fig 8 represents the daily THD_v change on node 46. Similar to the low penetration case, it can be observed that the THD_v is more when PVs inject power, and is less when EVs. Maximum and minimum THD_v obtained in this test case are approximately 3.6%, and 3%. THD_v are not of significant concern.

When the number of PVs increase, THD_i increases more when PVs inject power. However, it decreases when EVs are

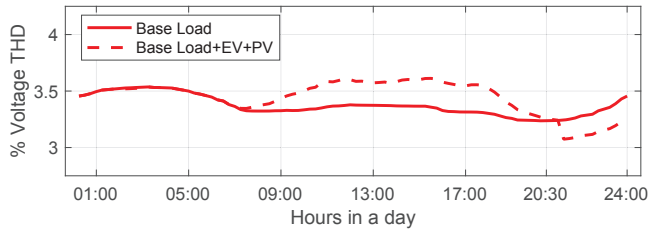

Fig. 8. Node 46 daily change of THD_v medium penetration level.

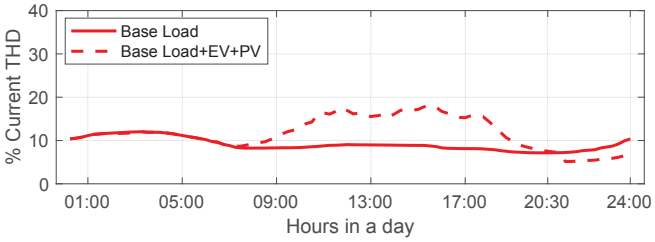

Fig. 9. Line 45-46 daily change of THD_i for medium penetration level.

charging (this is attributed to the definition of THD). This can easily be observed on Fig. 9 for node line 45-46 where the maximum THD_i jumped to an approximate value of 18%, and minimum THD_i dropped to an approximate value of 7%.

Similar results are observed for medium penetration level on 3 phases of node 7 as shown in Fig. 10. It can be observed that the increase in penetration level has higher rise of THD_v as compared to the rise of THD_v for low penetration level when PVs are injecting power. Similarly during the EVs charging, the decrease in THD_v due to EVs are more compared to low penetration level. However, since this node is close to substation the changes are lower compared to node 46.

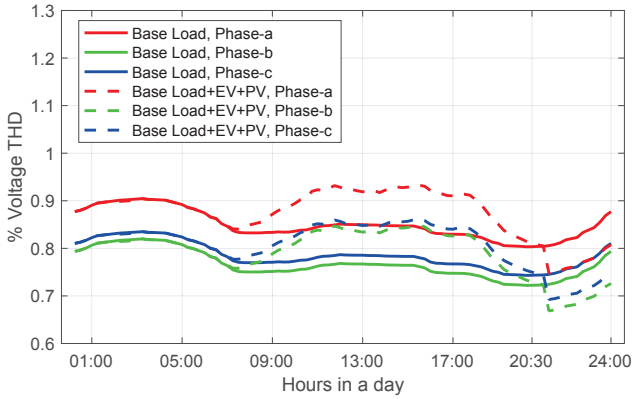

Fig. 10. Node 7 daily change of THD_v for 3 phases, medium penetration level.

C. High Penetration

Simulation results 100% penetration for node 46 are shown in Fig. 11 and Fig. 12 for THD_v and THD_i, respectively. It can be observed that the increases and decreases of THD_v during PV operations and charging of EVs are the highest. The results confirm the observations of the results observed for the low and medium penetration levels.

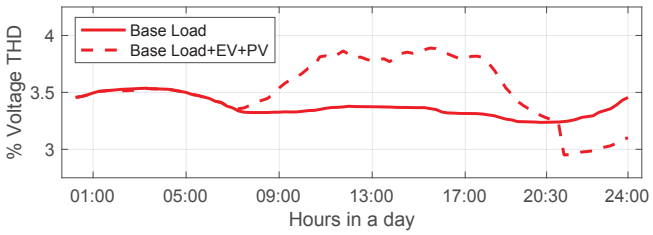

Fig. 11. Node 46 daily change of THD_v high penetration level.

Similar results are observed for THD_i in Fig. 12. From the figure, it can be observed that minimum and maximum THD_v are approximately 2.9% and 3.9%. The THD_v is not of concern even for higher penetration level of EVs/PVs. Similarly, these values are 5% and 33% for THD_i as observed from Fig. 12.

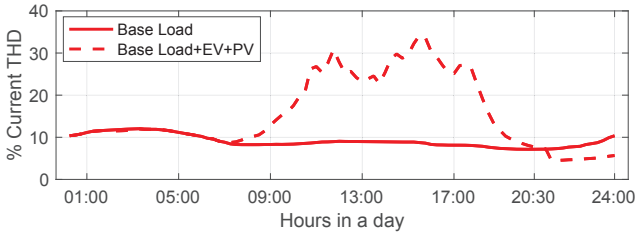

Fig. 12. Line 45-46 daily change of THD_i for high penetration level.

The THD_v values of node 7 for high penetration level is shown on Fig. 13. Compared to the results with medium and low penetration level, the maximum and minimum THD_v values are higher and lower, respectively.

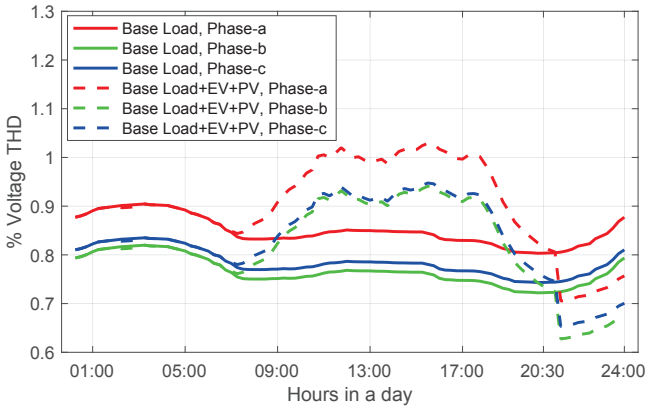

Fig. 13. Node 7 daily change of THD_v for 3 phases, high penetration level.

IV. Conclusion

This paper presented the harmonic assessment to understand the total impact of EVs and PVs on distribution systems. Simulations were carried out for low, medium, and high penetration levels, and results were presented for THD_v and THD_i for two selected nodes and lines on the medium voltage IEEE 123-node test feeder. It was observed that the harmonic voltages are becoming higher on nodes farther

away from substation. The impact on voltage and current harmonics increases as the level of penetration increases. When PVs are injecting power, both voltage and current harmonics increase. On the other hand, both voltage and current harmonics decrease when EVs are charging (due to the definition of THDs). From the results, it can be concluded that the existence of high number of PVs and EVs in future electricity distribution systems can create additional problems due to current harmonics; however, the voltage harmonics may not be much of a concern. Current harmonic issues could possibly be mitigated by coordinated charging of EVs and control of distributed PVs by using optimization approaches in a system with large pentration of EVs/PVs.

REFERENCES

[1] C. T. Li, C. Ahn, H. Peng, and J. Sun, "Synergistic control of plug-in vehicle charging and wind power scheduling," *IEEE Transactions on Power Systems*, vol. 28, no. 2, pp. 1113–1121, May 2013.

[2] A. Y. Saber and G. K. Venayagamoorthy, "Plug-in vehicles and renewable energy sources for cost and emission reductions," *IEEE Transactions on Industrial Electronics*, vol. 58, no. 4, pp. 1229–1238, April 2011.

[3] C.-T. Li, C. Ahn, H. Peng, and J. Sun, "Integration of plug-in electric vehicle charging and wind energy scheduling on electricity grid," in *Proc. Innovative Smart Grid Technologies Conference*, Jan 2012, pp. 1–7.

[4] S. H. Berisha, G. G. Karady, R. Ahmad, R. Hobbs, and D. Karner, "Current harmonics generated by electric vehicle battery chargers," in *Proc. of International Conference on Power Electronics, Drives and Energy Systems for Industrial Growth*, Jan 1996, pp. 584–589.

[5] IEC/TS 61000-3-4 ed1.0:1998. Electromagnetic compatibility (EMC) - Part 3-4: Limits - Limitation of emission of harmonic currents in lowvoltage power supply systems for equipment with rated current greater than 16 A.

[6] L. Kütt, E. Saarijärvi, M. Lehtonen, H. Mõlder, and J. Niitsoo, "A review of the harmonic and unbalance effects in electrical distribution networks due to EV charging," in *Proc. 12th International Conference on Environment and Electrical Engineering*, May 2013, pp. 556–561.

[7] "IEEE recommended practices and requirements for harmonic control in electrical power systems," *IEEE Std 519-1992*, pp. 1–112, April 1993.

[8] J. C. Gomez and M. M. Morcos, "Impact of EV battery chargers on the power quality of distribution systems," *IEEE Transactions on Power Delivery*, vol. 18, no. 3, pp. 975–981, July 2003.

[9] A. Lucas, F. Bonavitacola, E. Kotsakis, and G. Fulli, "Grid harmonic impact of multiple electric vehicle fast charging," *Electric Power Systems Research*, vol. 127, pp. 13 – 21, 2015.

[10] P. S. Moses, M. A. S. Masoum, and K. M. Smedley, "Harmonic losses and stresses of nonlinear three-phase distribution transformers serving plug-in electric vehicle charging stations," in *Proc. Innovative Smart Grid Technologies Conference*, Jan 2011, pp. 1–6.

[11] S. Deilami, A. S. Masoum, P. S. Moses, and M. A. S. Masoum, "Voltage profile and thd distortion of residential network with high penetration of plug-in electrical vehicles," in *Proc. Innovative Smart Grid Technologies Conference*, Oct 2010, pp. 1–6.

[12] M. A. S. Masoum, S. Deilami, and S. Islam, "Mitigation of harmonics in smart grids with high penetration of plug-in electric vehicles," in *IEEE PES General Meeting*, July 2010, pp. 1–6.

[13] M. Etezadi-Amoli, K. Choma, and J. Stefani, "Rapid-charge electric-vehicle stations," *IEEE Transactions on Power Delivery*, vol. 25, no. 3, pp. 1883–1887, July 2010.

[14] C. Jiang, R. Torquato, D. Salles, and W. Xu, "Method to assess the power quality impact of plug-in electric vehicles," in *Proc. International Conference on Harmonics and Quality of Power*, May 2014, pp. 177–180.

[15] A. Ul-Haq, C. Cecati, A. Ehsan, and K. Strunz, "Impact of electric vehicles on voltage profile and harmonics in a distribution network," in *Proc. First Workshop on Smart Grid and Renewable Energy*, March 2015, pp. 1–6.

[16] R. Bass, R. Harley, F. Lambert, V. Rajasekaran, and J. Pierce, "Residential harmonic loads and EV charging," in *2001 IEEE Power Engineering Society Winter Meeting*, vol. 2, 2001, pp. 803–808 vol.2.

[17] F. Lambert, *Secondary distribution impacts of residential electric vehicle charging*. California Energy Commission, Public Interest Energy Research Program, 2000.

[18] A. Chidurala, T. K. Saha, and N. Mithulananthan, "Harmonic impact of high penetration photovoltaic system on unbalanced distribution networks–learning from an urban photovoltaic network," *IET Renewable Power Generation*, vol. 10, no. 4, pp. 485–494, 2016.

[19] I. T. Papaioannou, A. S. Bouhouras, A. G. Marinopoulos, M. C. Alexiadis, C. S. Demoulias, and D. P. Labridis, "Harmonic impact of small photovoltaic systems connected to the LV distribution network," in *Proc. 5th International Conference on the European Electricity Market*, May 2008, pp. 1–6.

[20] P. T. Staats, W. M. Grady, A. Arapostathis, and R. S. Thallam, "A statistical method for predicting the net harmonic currents generated by a concentration of electric vehicle battery chargers," *IEEE Transactions on Power Delivery*, vol. 12, no. 3, pp. 1258–1266, Jul 1997.

[21] G. Carpinelli, G. Celli, S. Mocci, F. Pilo, and A. Russo, "Optimisation of embedded generation sizing and siting by using a double trade-off method," *IEE Proceedings - Generation, Transmission and Distribution*, vol. 152, no. 4, pp. 503–513, July 2005.

[22] O. Amanifar, "Optimal distributed generation placement and sizing for loss and THD reduction and voltage profile improvement in distribution systems using particle swarm optimization and sensitivity analysis," in *Proc. 16th Electrical Power Distribution Conference*, April 2011, pp. 1–7.

[23] M. Sedighi, A. Igderi, and A. Parastar, "Sitting and sizing of distributed generation in distribution network to improve of several parameters by pso algorithm," in *Proc. Conference Proceedings IPEC*, Oct 2010, pp. 1083–1087.

[24] Y. Alinejad-Beromi, M. Sedighizadeh, and M. Sadighi, "A particle swarm optimization for sitting and sizing of distributed generation in distribution network to improve voltage profile and reduce THD and losses," in *Proc. 43rd International Universities Power Engineering Conference*, Sept 2008, pp. 1–5.

[25] Y. Y. Hong and Y. T. Chen, "Three-phase optimal harmonic power flow," *IEE Proceedings - Generation, Transmission and Distribution*, vol. 143, no. 4, pp. 321–328, Jul 1996.

[26] Y.-Y. Hong, "Optimal harmonic power flow," *IEEE Transactions on Power Delivery*, vol. 12, no. 3, pp. 1267–1274, Jul 1997.

[27] A. Ulinuha, M. A. S. Masoum, and S. M. Islam, "Harmonic power flow calculations for a large power system with multiple nonlinear loads using decoupled approach," in *Proc. Australasian Universities Power Engineering Conference*, Dec 2007, pp. 1–6.

[28] "Modeling and simulation of the propagation of harmonics in electric power networks. II. sample systems and examples," *IEEE Transactions on Power Delivery*, vol. 11, no. 1, pp. 466–474, Jan 1996.

[29] S. Paudyal, C. A. Canizares, and K. Bhattacharya, "Optimal operation of distribution feeders in smart grids," *IEEE Transactions on Industrial Electronics*, vol. 58, no. 10, pp. 4495–4503, Oct 2011.

[30] M. A. S. Masoum, P. S. Moses, and S. Deilami, "Load management in smart grids considering harmonic distortion and transformer derating," in *Proc. Innovative Smart Grid Technologies Conference*, Jan 2010, pp. 1–7.

[31] G. Bharati and S. Paudyal, "Coordinated control of distribution grid and electric vehicle loads," *Electric Power Systems Research*, vol. 140, pp. 761 – 768, 2016.

[32] E. Cherian, G. Bindu, and P. C. Nair, "Pollution impact of residential loads on distribution system and prospects of DC distribution," *International Journal on Engineering Science and Technology*, vol. 19, no. 4, pp. 1655 – 1660, 2016.

[33] A. A. Latheef, "Harmonic impact of photovoltaic inverter systems on low and medium voltage distribution systems," Master's thesis, University of Wollongong, Australia, 2006.

[34] Electric Power Research Institute, "Simulation tool – OpenDSS," Available: http://smartgrid.epri.com/SimulationTool.aspx.

[35] IEEE Power & Energy Society, "Distribution test feeders," Available: http://ewh.ieee.org/soc/pes/dsacom/testfeeders/ .

[36] W. H. Kersting, "Radial distribution test feeders," in *Proc. Power Engineering Society Winter Meeting*, vol. 2, 2001, pp. 908–912.